

**SCREENING FOR POTENTIAL INHIBITORS OF
MYCOBACTERIUM TUBERCULOSIS
ISOCITRATE LYASE:
IN SILICO AND *IN VITRO* APPROACHES**

LEE YIE VERN

UNIVERSITI SAINS MALAYSIA

2017

**SCREENING FOR POTENTIAL INHIBITORS OF
MYCOBACTERIUM TUBERCULOSIS
ISOCITRATE LYASE:
IN SILICO AND IN VITRO APPROACHES**

by

LEE YIE VERN

**Thesis submitted in fulfilment of the requirements
for the degree of
Doctor of Philosophy**

November 2017

ACKNOWLEDGEMENT

It has been a long journey to complete this PhD project, so many people to thank.

First, I would like to acknowledge Ministry of Science, Technology and Innovation for kind scholarship support, National Science Fellowship. Also their kind financial support for my oversea internship in Japan. My heart-felt appreciation to all staffs in Univesiti Sains Malaysia and INFORMM who have helped me throughout my study.

My greatest gratitude goes to my supervisor, Dr. Choong Yee Siew. Thank you for your patience and support in my journey. I would not be able to complete this without you. For the time I almost give up, thanks for your guidance, encouragement, motivation, believing and trust. You always secured me by being there for me. I would like to acknowledge and appreciate all you have done for me.

Next, I would like to thank my co-supervisor Prof. Habibah for welcoming me to the team and met my supervisor Dr. Choong Yee Siew. Besides, thanks for her arrangement for my internship in Osaka University in Japan with Prof. Hideo Matsuda. Thank you for all the resources and opportunities that you have given to me. You made me always remember to be humble in front of knowledge.

I also would like to take this opportunity to express my appreciation to co-supervisor Dr. Lim Theam Soon. Thank you for your advices and helping hand when I almost drown in my depression. You are always the light of hope when I am desperate. Not to be forgotten you have bring me to Prof. Armando and Prof. Maria when I have no one to turn to for technical advices.

It is my pleasure and honour to have so many help in my study. I am so grateful to Prof. Hideo Matsuda for willing to accept me as intern in his lab and his kind offer on computational resources. Also, much appreciated for Prof. Armando and Prof. Maria advices to culture *M. smegmatis*. Dr How Siew Eng and Dr Lee Ping Chin from Universiti Malaysia Sabah also provided much help for sharing their *M. smegmatis* strain. Last but not least, I would like to thank Dr. Sasidharan advices on in disc diffusion assay; Prof. Gurjeet advices on microscope usage; Dr. Radmad Zakaria and Mr. Shun from Herbarium USM for their assistance to complete the voucher specimen; Dr. Choi Sy Bing and Dr. Yam Wai Keat for being my kind senior and mentor when I first entering this field of study.

My life of study will not be that interesting without my lovely lab mates: Syazana, Tommy Yap, Roy Lee, Kevin Khoo, Bee Yin, Michael Law, Jia Xin and Chai Fen. Also spices of life have been added by a bunch of friends in INFORMM especially Bee Nar, Hidayah, Mimie, Siang Tean, QuiTing, Soo Khim, Chai Fung, Angela Ch'ng, Hamizah, Anizah, Shin Yong, Kelvin Lew and Slyvia. I miss the time we have fun together. Do keep in touch and take care.

My degree of PhD is my sincere thanksgiving present for my parents and family members who have given me countless mental support for so many years. I am indebted to my parents for letting me to do what I like to do for my life. Without their love and support, I could not make everything possible.

Lastly, I would like to dedicate everything I have now to my beloved husband, Kelvin Kong Hong Guan for his support whenever I broke down in tears. Thank you for his accompany, understanding and love he has given me, grooming me to a better person.

TABLE OF CONTENTS

ACKNOWLEDGEMENT	ii
TABLE OF CONTENTS	iv
LIST OF TABLE	viii
LIST OF FIGURE	x
LIST OF ABBREVIATIONS	xvi
LIST OF SYMBOLS	xix
ABSTRAK	xx
ABSTRACT	xxii

CHAPTER 1

GENERAL OVERVIEW

1.1 Statement of the problem.....	1
1.2 General objective of the study	1
1.3 Tuberculosis.....	2
1.3.1 Tuberculosis infection	3
1.3.2 Drug resistance of <i>Mycobacterium tuberculosis</i>	5
1.3.3 <i>Mycobacterium tuberculosis</i> in dormancy.....	7
1.3.4 Isocitrate lyase as drug target	8
1.3.5 Isocitrate lyase related studies	10
1.4 Protein study	29
1.4.1 Protein dynamics	29
1.4.2 Molecular Dynamics Simulation	30
1.4.3 Virtual screening (VS).....	34
1.4.4 High-throughput screening	37
1.5 Medicinal plants	38

CHAPTER 2

MOLECULAR DYNAMICS SIMULATION FOR ISOCITRATE LYASE

2.1 Introduction	39
2.2 Fundamental of molecular dynamics simulation.....	41
2.2.1 Energy minimization	41

2.2.2	Molecular mechanics	43
2.3	Specific Objective.....	49
2.4	Methodology.....	51
2.4.1	Setting up the system for molecular dynamics simulation	51
2.4.2	Equilibration of the system.....	53
2.4.3	Free energy calculation.....	53
2.5	Result.....	55
2.5.1	System stability.....	55
2.5.2	Root mean square deviation (RMSD) analysis.....	58
2.5.3	Root mean square fluctuation (RMSF) analysis.....	61
2.5.4	Principle component analysis	66
2.5.5	Free energy calculation (MM-PBSA/GBSA analysis).....	71
2.5.6	Radial distribution function and hydrogen bond analysis	74
2.6	Discussion.....	77
2.7	Conclusion	81

CHAPTER 3

ENSEMBLE DOCKING FOR ISOCITRATE LYASE

3.1	Introduction	82
3.2	Ensemble Conformation	82
3.2.1	Clustering of protein trajectories	83
3.3	Molecular docking simulation	83
3.3.1	Degree of freedom in molecular docking	84
3.3.2	Docking algorithm.....	84
3.3.3	Free energy of binding in molecular docking.....	86
3.3.4	Scoring function	86
3.4	Ensemble docking.....	88
3.4.1	Virtual screening (VS).....	88
3.5	Specific Objective.....	90
3.6	Methodology.....	90
3.6.1	Ensemble conformation.....	90
3.6.2	Ensemble Docking (Virtual Screening).....	91
3.7	Result.....	91

3.7.1	Clustering analysis.....	91
3.7.2	Ensemble docking (Virtual screening)	95
3.8	Discussion.....	104
3.9	Conclusion.....	105

CHAPTER 4

ENZYMATIC ASSAY FOR ISOCITRATE LYASE POTENTIAL INHIBITOR

4.1	Introduction	106
4.1.1	High-throughput screening	106
4.1.2	Isocitrate lyase related studies - inhibitor studies related to ICL	107
4.1.3	Enzymatic assay	108
4.2	Specific objective	113
4.3	Methodology.....	113
4.3.1	Compound or crude extract preparation	113
4.3.2	Voucher specimen	117
4.3.3	Cloning and expression of ICL.....	119
4.3.4	Extraction and purification of ICL	125
4.3.5	Western Blot	127
4.3.6	Enzymatic assay	128
4.4	Result.....	130
4.4.1	Voucher specimen	130
4.4.2	Cloning and expression of ICL.....	130
4.4.3	Extraction and purification of ICL	140
4.4.4	Enzymatic assay	142
4.5	Discussion.....	153
4.6	Conclusion.....	158

CHAPTER 5

WHOLE CELL ASSAY SCREENING FOR ISOCITRATE LYASE POTENTIAL INHIBITOR

5.1	Introduction	159
5.1.1	High content screening (HCS).....	159
5.1.2	Isocitrate lyase related studies - Inhibitor studies related to non-MTB ICL.....	160

5.2	Specific objectives	161
5.3	Methodology.....	162
5.3.1	<i>Mycobacterium smegmatis</i>	162
5.3.2	Whole cell assay	166
5.3.3	Minimum inhibitory concentration.....	167
5.3.4	Minimum bactericidal concentration.....	169
5.4	Result.....	169
5.4.1	<i>Mycobacterium smegmatis</i>	169
5.4.2	Whole cell assay	176
5.4.3	Minimum inhibitory concentration.....	178
5.4.4	Minimum bactericidal concentration.....	180
5.5	Discussion.....	183
5.6	Conclusion	186

CHAPTER 6

GENERAL CONCLUSION

6.1	Concluding remarks.....	188
6.2	Limitations.....	190
6.3	Future Works	191

REFERENCES

APPENDICES

LIST OF PUBLICATION

LIST OF TABLE

		Page
Table 1.1	Summary of synthetic and natural potential inhibitor for MTB ICL and non-MTB ICL.	14
Table 2.1	Detail information of the ICL systems.	53
Table 2.2	The information of ICL residues.	57
Table 2.3	Highest eigenvalue in each nano-second (2 – 30) of MD simulation for Apo_ICL.	67
Table 2.4	Highest eigenvalue in each nano-second (2 – 30) of MD simulation for Complex1_ICL.	68
Table 2.5	Highest eigenvalue in each nano-second (2 – 30) of MD simulation for Complex2_ICL.	69
Table 2.6	Weight percentage of highest eigenvalue of each active site.	70
Table 2.7	Binding free energy of Complex1_ICL and Complex2_ICL system.	73
Table 2.8	Hydrogen bond occupancy for three ICL systems.	76
Table 3.1	The number of clusters for three MD systems. Selected cluster radius is highlighted in bold.	93
Table 3.2	Summary of ICL ensemble conformations contributed from three MD simulation.	94
Table 3.3	Binding free energy of the control dockings.	97
Table 3.4	Grid center of each ensemble conformations.	97
Table 3.5	Lipinski's Rule of Five. (Lipinski <i>et al.</i> , 2001)	99
Table 3.6	The 22 compounds concluded from ensemble docking as ICL potential inhibitor.	100
Table 4.1	PCR reaction mix.	122
Table 4.2	PCR protocol.	122
Table 4.3	Ligation mix to ligate MTB ICL and pET28a.	134
Table 4.4	Transformation of ligated product into DH10 β .	136

Table 4.5	Rate of reaction, enzyme activity and specific activity of ICL at different concentration of isocitrate.	144
Table 4.6	NADH absorbance at 340nm for 5 min at different DF of ICL.	145
Table 4.7	NADH absorbance at 340 nm at 5 min with different concentration of isocitrate.	147
Table 4.8	1/[S] and 1/V value for Lineweaver plot.	150
Table 5.1	Composition of control and test wells for MIC study on <i>M. smegmatis</i> .	168
Table 5.2	MIC of the crude extracts and respective suggested compounds.	179

LIST OF FIGURE

		Page
Figure 1.1	Summary of <i>Mycobacterium tuberculosis</i> life cycle in human host.	4
Figure 1.2	The Krebs cycle and the glyoxylate pathway for energy generation. The blue bold arrow indicates the Krebs cycle and the red arrow shows the glyoxylate bypass.	9
Figure 1.3	The structure of ICL from MTB. a) Tetramer, each colour represents a subunit of ICL; b) dimer, cyan and orange represents monomer 1 and monomer 2; c) dimer in open conformation; d) ICL dimer in close conformation; e) monomer 1 in open conformation without ligand; and e) monomer 1 in close conformation with ligand. Purple represents the active site (Sharma <i>et al.</i> , 2000; Lee <i>et al.</i> , 2015).	11
Figure 2.1	Energy of a biological system as a function of time.	42
Figure 2.2	The Lennard Jones 12-6 potential. The σ stands collision diameter and ϵ stands for well depth. The r_m is the minimum radius of the molecules.	47
Figure 2.3	Periodic boundary condition in two dimensions (ISSACS, 2010).	50
Figure 2.4	Monomer 1 of ICL. a) Apo_ICL in open conformation, b) Complex1_ICL in close conformation and c) Complex2_ICL in close conformation. Purple represents the active site.	53
Figure 2.5	Active site of ICL. a) Apo_ICL in open conformation without ligand, b) Complex1_ICL in close conformation with glyoxylate/succinate and c) Complex2_ICL in close conformation with isocitrate.	53
Figure 2.6	ICL active site of a) Apo_ICL, b) Complex1_ICL and c) Complex2_ICL. In a1, b1 and c1, the transparent blue represents the monomer 1, the transparent orange represents the monomer 2 and the purple represents the active site. In a2, b2 and c2, the green represents the entrance gate and the orange represents the C-terminal of monomer 2 that acts as a weight on top of the entrance gate.	56
Figure 2.7	Superimpose of ICL active site. a) Apo_ICL in purple, b) Complex1_ICL in cyan. The green represents the entrance gate in open conformation whereas the blue represents the entrance gate in close conformation. The orange	56

represents the C-terminal loop of monomer 2 in open conformation and the brown represents the C-terminal loop of monomer 2 in close conformation.

- Figure 2.8 RMSD of (a) Apo_ICL; (b) Complex1_ICL; (c) Complex2_ICL during 30 ns MD simulation. Black and red line represent RMSD of ICL dimer (854 residues) and active site (147 residues), respectively. Green and blue line represent RMSD of active site 1 and 2, respectively. 59
- Figure 2.9 Active loop and terminal loop RMSD of (a) Apo_ICL; (b) Complex1_ICL; (c) Complex2_ICL during 30 ns MD simulation. Black and red lines represent RMSD of ICL active site 1 and 2, respectively. Green and blue lines represent RMSD of C-terminal loop 1 and 2, respectively. Yellow and pink lines represent RMSD of N-terminal loop 1 and 2, respectively. 60
- Figure 2.10 RMSF of (a) Apo_ICL, (b) Complex1_ICL and (c) Complex2_ICL throughout 30 ns MD simulation. Black line indicates the average RMSF. The high RMSD residue in red circle indicates C-terminal residues. 62
- Figure 2.11 Active site RMSF of a) Apo_ICL, b) Complex1_ICL, and c) Complex2_ICL throughout 30ns MD simulation. Black arrow indicates the active site residues of both active sites. The coloured arrows are the location of loops: Red (residues 91-93); Yellow (residues 104-114); Green (residues 154-159); Pink, the entrance gate (residues 185-196); Cyan (residues 230-234); Purple (residues 285-289); Ice-blue (residues 314-319). 64
- Figure 2.12 Active site of ICL dimer with ligand at final 30 ns MD simulation. a) Complex1_ICL active site 1, b) Complex1_ICL active site 2, c) Complex2_ICL active site 1 and d) Complex2_ICL active site 2. Loops were highlighted in colours with respective active site 1/active site 2 residue number. Red: residues 91-93/518-520; Yellow: residues 104-114/531-541; Green: residues 154-159/581-585; Pink: residues 185-196/612-623; Cyan: residues 230-234/657-661; Purple: residues 285-289/712-716; Ice-blue: residues 314-319/741-746. 65
- Figure 2.13 Porcupine plot of highest eigenvalue eigenvector of each active site for (a) active site of Apo_ICL 1, (b) active site of Complex1_ICL and (c) active site of Complex2_ICL. Red arrow summarized the vector and magnitude of motion. 72
- Figure 2.14 Radial distribution function of water for a) Complex1_ICL and b) Complex2_ICL. 75

Figure 3.1	Control docking of ICL X-rays crystal structure. a) ICL close conformation (PDB id: 1F8I) shown as red and b) ICL open conformation (PDB id: 1F61) shown in blue. Ligand succinate, glyoxylate and isocitrate shown in licorice representation. In close conformation, figure shows that succinate and glyoxylate was nicely fit back to active site. Whereas in open conformation, succinate and glyoxylate cannot fit well in the active site. Additional docking was carried out for isocitrate. Isocitrate binding was satisfied for both active site.	96
Figure 3.2	Docking of all three ligands into MD structure. a) Apo_ICL in orange colour (superimposed with open conformation of ICL crystal structure), b) Complex1_ICL in green and c) Complex2_ICL in purple colour (superimposed with close conformation of ICL crystal structure). Ligand succinate, glyoxylate, and isocitrate are shown in CPK representation, respectively.	96
Figure 4.1	Lineweaver-burk plot (Lineweaver and Burk, 1934).	112
Figure 4.2	Example of chemical compound information in NADI database.	114
Figure 4.3	Example of specimen label.	118
Figure 4.4	Process of voucher specimen preparation for asam jawa plant. (a) Collection of plant specimen, (b) immobilized on paper, (c) sterilized with alcohol in plastic storage bag, (d)/(e) pressed with plant press, (f) dried fruit in oven, (g) mounted plant specimen on herbarium sheet.	118
Figure 4.5	Gene sequence of MTB ICL. (GenBank accession number: AL123456.3)	131
Figure 4.6	Vector map of pET28a (Novagen).	131
Figure 4.7	Gel electrophoresis of PCR amplified MTB ICL from plasmid PM107. a) Promega 1Kb DNA ladder. b) The correct band size of 1287 bp was amplified.	133
Figure 4.8	Gel electrophoresis of digested pET28a. The correct band size of 5344 bp was obtained.	133
Figure 4.9	Control experiment for transformation of MTB ICL into DH10 β . a) Positive control - undigested pET28a, b) negative control – DH10 β , c) negative control – no ligase, d) negative control – no ICL and e) negative control – no pET28a.	137

Figure 4.10	Transformation of MTB ICL into DH10 β . a) 3:1 sample, b) 5:1 sample, 3:1 concentrated sample and d) 5:1 concentrated sample.	138
Figure 4.11	Gel electrophoresis for colony PCR. Lane 1: 1kb DNA ladder; lane 2: PCR of PM107 plasmid amplified MTB ICL within (1287 bp); Clone #3, 4, 6, 12, 13, 14, 15. 16. 17 were positive clone (1600 bp). Clone #13 was selected for expression.	139
Figure 4.12	Transformation of clone #13 into expression vector <i>E. coli</i> BL21.	139
Figure 4.13	SDS-PAGE of BL21-ICL. Lane 1: 1 kDa protein ladder; Lane 2: BL21-ICL pellet; Lane 3: BL21-ICL supernatant; Lane 4: flow through 1 (F1); Lane 5: wash 1 (W1), Lane 6: wash 2 (W2); Lane 7: elution 1 (E1); Lane 8: elution 2 (E2); Lane 9: elution 3 (E3); Lane 10: elution 4 (E4). MTB ICL have weight about 50 kDa. MTB ICL for E1 is about 6.8 mg/ml.	141
Figure 4.14	Western blot of BL21-ICL. Lane 1: 1 kDa protein ladder; Lane 2: BL21-ICL pellet; Lane 3: BL21-ICL supernatant; Lane 4: flow through 1 (F1); Lane 5: wash 1 (W1), Lane 6: wash 2 (W2); Lane 7: elution 1 (E1); Lane 8: elution 2 (E2); Lane 9: elution 3 (E3); Lane 10: elution 4 (E4). The purified MTB ICL is specifically bound to anti-His-HRP and developed by CN/DAB substrate.	141
Figure 4.15	NADH absorbance at 340 nm throughout 5 min enzymatic assay for ICL DF a) 0.5, b) 0.25 and c) 0.125. ICL DF 0.125 was proven to be sufficient for assay use.	146
Figure 4.16	NADH Absorbance 340 nm throughout 5 min at different isocitrate concentration. Rate of reaction was obtained by calculating the slope of the graph.	148
Figure 4.17	Lineweaver-burk plot of ICL.	150
Figure 4.18	NADH absorbance at 340 nm for 5 min throughout the ICL inhibitory assay. a) Catechin, b) L- minosine, c) adenosine, d) citric acid, e) quinic acid, f) glucose and g) itaconate (positive control). Blue line indicate the negative control and black line is the pure compound.	151
Figure 4.19	NADH absorbance at 340 nm for 5 min throughout the ICL inhibitory assay. a) Tebu, b) cili, c) ciku d) peria, e) asam jawa, f) asam gelugor, g) mengkudu, h) lemuni, i) ketum and j) delima. Blue line indicate the negative control and black line is the crude extract.	152

Figure 4.20	The graph appearance for a typical continuous enzymatic assay. The initial rate of reaction indicated by the linear line. The dash line is not included for the initial rate of reaction calculation.	156
Figure 4.21	The graph appearance for a substance disappearance within a continuous enzymatic assay. Dash line shows that the enzyme is too diluted, bold linear line indicate the enzyme is in appropriate dilution and curve line indicate that the enzyme is too concentrated.	156
Figure 5.1	The morphology of (a) <i>M. smegmatis</i> and (b) <i>E. coli</i> from acid fast staining.	171
Figure 5.2	Spot inoculate of <i>M. smegmatis</i> inoculum on M9 minimal agar with a) 0.4% and b) 0.1% carbon source. A1-A4 are inoculum in Middlebrook 7H9 with ADC enrichment, B1-B4 are inoculum in M9 minimal media with acetate and C1-C4 are inoculum in M9 minimal media with glucose.	173
Figure 5.3	M9 minimal agar plates with <i>M. smegmatis</i> seed culture of a) OD _{600nm} of 0.1 and b) OD _{600nm} of 1.0. No mycobacterium growth observed after incubated at 37°C for 3 days, regardless of bacterium spreading method.	175
Figure 5.4	a) M9 minimal agar plates with <i>M. smegmatis</i> seed culture of OD _{600nm} of 2.0 and 2.6 with different type of spreading method, as well as b) seed culture of OD _{600nm} of 1.5 with spreading method of pre dip the cotton swab and loaded with 100 µl of seed culture.	175
Figure 5.5	Positive control (a) kanamycin, (b) itaconate and negative control (c) sterile water and (d) 100% DMSO of disc diffusion assay for <i>M. smegmatis</i> .	177
Figure 5.6	Pure compound (a) (+) – catechin, (b) L- minosine, (c) glucose, (d) adenosine, (e) citric acid and (f) quinic acid in disc diffusion assay for <i>M. smegmatis</i> .	177
Figure 5.7	Disc diffusion assay for (a) <i>M. zapota</i> , (b) <i>M. citrifolia</i> , (c) <i>V. negundo</i> and (d) <i>M. charantia</i> . (e) <i>C. annuum</i> , (f) <i>S. officinarum</i> , (g) <i>M. speciose</i> , (h) <i>T. indica</i> , (i) <i>G. atroviridis</i> and (j) <i>P. granatum</i> for <i>M. smegmatis</i> .	177
Figure 5.8	MBC test for <i>M. smegmatis</i> in itaconate. MBC is 6.25 mg/ml. Results were in triplicate.	181

Figure 5.9	MBC test for <i>M. smegmatis</i> in a) <i>M. zapota</i> and b) <i>M. citrifolia</i> . Both extracts have MBC value of 25 mg/ml. Results were in triplicate.	181
Figure 5.10	MBC test for <i>M. smegmatis</i> in <i>V. negundo</i> . MBC is 1.6 mg/ml. Results were in triplicate.	181
Figure 5.11	MBC test for <i>M. smegmatis</i> in <i>M. charantia</i> . MBC is 1.6 mg/ml. Results were in triplicate.	182
Figure 5.12	Control set for MBC of <i>M. smegmatis</i> . (a) <i>M. zapota</i> and <i>M. citrifolia</i> , (b) itaconate, (c) <i>V. negundo</i> and (d) <i>M. charantia</i> . No <i>M. smegmatis</i> growth was observed indicating that itaconate, crude extracts and broths were not contaminated. Addition control (e) for MS + H ₂ O, MS + DMSO, M9 control (M9 broth only), MS + kana (<i>M. smegmatis</i> with kanamycin) and M9 + MS control (M9 broth with <i>M. smegmatis</i>) shows that water and 100% DMSO did not inhibit it, the M9 broth was free from contamination, as well as the inoculum still is kanamycin sensitive <i>M. smegmatis</i> .	182

LIST OF ABBREVIATIONS

ADC	Albumin Dextrose Catalase
ADMET	Adsorption, Distribution, Metabolism, Excretion and Toxicity
AIDS	Acquired Immune Deficiency Syndrome
ALA	Alanine
AMBER	Assisted Model Building with Energy Refinement
AR	Analytical Reagent
ARG	Arginine
ASN	Asparagine
ASP	Aspartic Acid
ATCC	American Type Culture Collection
BCG	Bacillus Calmette-Guérin
CaCl ₂	Calcium Chloride
CHARMM	Chemistry at Harvard Macromolecular Mechanics
CPK	Corey-Pauling-Koltun
CYS	Cysteine
dH ₂ O	Distilled Water
DMSO	Dimethyl Sulfoxide
Eq	Equation
FF	Force Field
GA	Genetic Algorithm
GB	Generalized Born
GLN	Glutamine
GLU	Glutamic Acid
GLY	Glycine
GROMOS	Groningen Molecular Simulation Computer Program Package
HCS	High Content Screening
HIS	Histidine
HIV	Human Immunodeficiency Virus
HTS	High-throughput Screening

ICL	Isocitrate Lyase
IFU	Instruction For Use
ILE	Isoleucine
LCPO	Linear Combinations of Pairwise Overlaps
LEU	Leucine
LGA	Lamarkien Generic Algorithm
LJ	Lowenstein-Jensen
LYS	Lysine
MBC	Minimum Bactericidal Concentration
MD	Molecular Dynamics
MDR	Multidrug Resistant Strain
MET	Methionine
Mg	Magnesium
MgSO ₄	Magnesium Sulphate
MIC	Minimum Inhibitory Concentration
MM	Molecular Mechanics
MM-PBSA/GBSA	Molecular Mechanics Poisson-Boltzmann Surface Area/ Generalized Born Surface Area
MMTSB	Multiscale Modeling Tools for Structural Biology
MRC	Multiple Receptor Conformations
MS	Malate synthase
MTB	Mycobacterium tuberculosis
MTP	Micortiter Plates
Na	Sodium
NADI	Natural Product Discovery System
NMR	Nuclear Magnetic Resonance
NPT	Constant Number of Substance, Pressure, Temperature
NVE	Constant number of Substance, Volume, Energy
NVT	Constant number of Substance, Volume, Temperature
OADC	Oleic Albumin Dextrose Catalase
OD	Optical Density
PCA	Principal Component Analysis
PDB	Protein Data Bank

PHE	Phenylalanine
PRMT1	Protein Arginine Methyltransferase 1
PRO	Proline
PTP1B	Protein Tyrosine Phosphate 1B
QM	Quantum Mechanics
RMSD	Root Mean Square Deviation
RMSF	Root Mean Square Fluctuation
SA	Simulated Annealing
SASA	Solvent-Accessible Surface Area
SER	Serine
TAACF	Tuberculosis Antimicrobial Acquisition and Coordinating Facility
TB	Tuberculosis
TCA	Tricarboxylic Acid
TDR	Totally Drug Resistant
THR	Threonine
TIP3PBOX	Transferable Intermolecular Potential Three Point Water Box
TRP	Tryptophan
TYR	Tyrosine
uHTS	Ultra High-Throughput Screening
VAL	Valine
VS	Virtual Screening
WHO	World Health Organization
XDR	Extensively Drug Resistant

LIST OF SYMBOLS

Å	Angstrom
%	Percent
ΔG	Free energy of binding
ΔG_{ELE}	Electrostatic interaction energy
ΔG_{PB}	Polar solvation free energy
µg	Microgram
µl	Microliter
µm	Micro-meter
fs	Femto-second
g	Gram
K	Kelvin
Kcal	Kilo-calorie
L	Liter
logP	Logarithm of the partition coefficient
M	Molar
mg	Milligram
ml	Milliliter
mm	Millimeter
nm	Nano-meter
ns	Nano-second
°	Degree
°C	Degree Celsius
ps	Pico-second
rpm	Revolution per minute
α	Alpha
β	Beta

**PENYARINGAN PERENCAT BERPOTENSI UNTUK PERENCATAN
ISOCITRATE LYASE *MYCOBACTERIUM TUBERCULOSIS*:
PENDEKATAN *IN SILICO* DAN *IN VITRO***

ABSTRAK

Tuberkulosis (juga dikenali sebagai penyakit batuk kering atau penyakit tibi) merupakan sejenis penyakit yang dijangkit oleh bakteria *Mycobacterium tuberculosis* (MTB). Wabak global ini telah menjangkiti satu per tiga populasi dunia tanpa mengira jenis jangkitan aktif atau laten. Dalam dua jenis jangkitan ini, MTB menjalani metabolisme yang berbeza. Contohnya mereka mempunyai kitaran janaan tenaga yang berbeza semasa aktif dan laten. Bukannya menyasarkan sasaran ubat yang terlibat dalam metabolisme semasa MTB aktif, penyelidikan ini menyasarkan isocitrate lyase (ICL), satu sasaran ubat yang terlibat dalam kitaran janaan tenaga semasa MTB dalam keadaan dorman (juga dikenali sebagai glyoxylate cycle). Kajian sebelum ini menunjukkan bahawa MTB yang dorman tidak dapat hidup dalam paru-paru model tikus tanpa ICL. Pada masa yang sama, ICL tidak wujud dalam mamalia. Jadi, ICL adalah sesuai digunakan sebagai sasaran ubat. Dalam kajian ini, simulasi dinamik molekul (MD, molecular simulation) dilakukan ke atas struktur kristal ICL terlebih dahulu dengan pakej AMBER 8. Hasil daripada 30 ns simulasi MD telah menunjukkan bahawa lingkaran C-termina terlibat dalam jalan masuk ke tapak aktif. Melalui pengiraan MM-PBSA, didapati bahawa pengikatan substrat (isocitrate) adalah disumbangi oleh interaksi electrostatik dan hidrofobik. Kesatuan konformasi ICL yang dikumpul melalui simulasi MD telah digunakan untuk menyaring 3,000 kompaun kimia daripada tumbuhan tempatan Malaysia (NADI database). Penyaringan maya ini dilakukan dengan program AutoDock 3.05. Adalah didapati bahawa 22 calon

berpotensi telah memenuhi syarat Lipinski's Rule of Five (kriteria obat-rupa). Dalam 22 calon berpotensi, 6 boleh didapati secara komersil sebagai kompoun tulen malah 16 yang lain hanya boleh didapati melalui 12 tumbuhan (akhirnya hanya 10 tumbuhan sahaja yang didapati). Jadi 6 kompoun tulen dan 10 ekstrak tumbuhan telah digunakan dalam ujian aktiviti perencatan iaitu ujian enzim dan ujian disk difusi. Ujian enzim dilakukan dengan mengguna MTB ICL yang diklon, diekspres dan ditulen malah ujian disk difusi mengguna model gantian MTB, iaitu *M. smegmatis* untuk menguji perencat ICL yang berpotensi cadangan penyaringan maya. Namun itaconate, perencet ICL yang diketahui dapat menunjuk aktiviti perenjatan, tetapi kompoun tulen dan ekstrak tumbuhan tidak. Dalam ujian disk difusi, empat ekstrak telah menunjukkan perenjatan aktiviti ICL iaitu ekstrak *Manilkara zapota*, *Momordica charantia*, *Vitex negundo* dan *Morinda citrifolia*, dengan kepekatan renjatan minima (MIC, minimum inhibitory concentration) masing-masing sebanyak 12.5 mg/ml, 12 mg/ml, 0.78 mg/ml dan 0.39 mg/ml. Kepekatan baktericida minima *M. zapota* dan *M. charantia* adalah 25 mg/ml. Malah kepekatan baktericida minima *V. negundo* dan *M. citrifolia* adalah 1.6 mg/ml. Kombinasi eksperimen *in silico* dan *in vitro* ini telah berjaya mengenal pasti perencat MTB ICL yang berpotensi. Akan tetapi, pengoptimuman juga diperlukan untuk siasatan lanjut, contohnya pengajian aktiviti perencatan dengan ekstrak pecahan, pengenalan pasti kompoun yang terlibat dalam perencatan dan ujian lanjut atas kepekatan ekstrak yang berbeza dalam ujian enzim.

**SCREENING FOR POTENTIAL INHIBITORS OF
MYCOBACTERIUM TUBERCULOSIS ISOCITRATE LYASE:
IN SILICO AND IN VITRO APPROACHES**

ABSTRACT

Tuberculosis (TB) that is caused by *Mycobacterium tuberculosis* (MTB) still remains as global epidemic and affects one-third of the world population, regardless of active TB or latent TB infection. The metabolism for active and latent MTB are different, for instance they have different energy generation cycle during active and latent stage. Instead of focusing on the drug targets during the active stage, which already have the effective therapeutic drugs, this study targeted isocitrate lyase (ICL), a potential target for dormant (latent) MTB energy generation cycle (glyoxylate cycle). Studies showed that without ICL, dormant MTB cannot survive within the lung of a murine model. Besides, this enzyme is not found in mammals hence it is an appropriate drug target to eliminate TB. In this study, molecular dynamics (MD) simulations were first performed on the crystal structure of ICL, using AMBER 8 molecular dynamics package. Results from 30 ns of MD simulations showed that C-terminal loop is involved in the access towards the active site. In addition, MM-PBSA calculation showed that the substrate (isocitrate) binding was contributed by electrostatic interaction as well as the hydrophobic interactions. Ensemble conformations obtained from MD simulation were then used for virtual screening to search for the potential ICL inhibitor from Malaysian local plant database (NADI) with the collection of 3,000 compounds. Virtual screening that performed with AutoDock 3.05 has managed to identify 22 potential candidates which are within Lipinski's Rule of Five (with drug-likeness criteria). Of the 22 candidates, 6 were commercially available as pure

compound while the remaining 16 candidates can only be obtained from 12 plants (however, only 10 plants were available during the study). Therefore, 6 pure compounds and 10 crude extracts were used to test for their inhibition activity by enzymatic assay and disc diffusion assay. In enzymatic inhibitory assay, MTB ICL was cloned, expressed and purified whereas disc diffusion assay used a replacing MTB model, *M. smegmatis* to test against the potential inhibitors suggested from virtual screening. The known inhibitors of ICL, itaconate managed to show inhibition in enzyme inhibitory assay but the pure compounds and crude extracts were not. Astonishingly, four crude extracts: *Manilkara zapota*, *Momordica charantia*, *Vitex negundo* and *Morinda citrifolia* showed inhibitory effect on *M. smegmatis* with minimal inhibitory concentration (MIC) of 12.5 mg/ml, 12 mg/ml, 0.78 mg/ml and 0.39 mg/ml, respectively. *M. zapota* and *M. charantia* obtained minimal bactericidal concentration (MBC) of 25 mg/ml whereas *V. negundo* and *M. citrifolia* have MBC of 1.6 mg/ml. The combination of both *in silico* and *in vitro* approaches managed to identify potential compounds for MTB ICL. However, optimization will be needed in future study e.g. inhibition study on the fractionated crude extract, identification of compounds that gave inhibition effects and further testing on different concentration of crude extract for enzymatic assay.

CHAPTER ONE

GENERAL OVERVIEW

1.1 Statement of the problem

It is indisputable that *Mycobacterium tuberculosis* (MTB) is a resurgent infectious disease. Compounded to the problem are the multidrug resistant, extensively drug resistant strains and totally drug resistant strains. The development of current potential drugs, which mainly target on active phase MTB, is bound to face a certain extent of challenges when the drugs are no longer effective against the targets. The research on new drug target and new source of drug has thus become tougher and time consuming. This could be one of the reasons for no new treatment regime available since 40 years ago. In addition, no drug has been developed to target on latent phase MTB. If new drug can target on dormant phase MTB, TB dormancy might be able to be eradicated.

1.2 General objective of the study

The initial part of this study was to investigate the dynamics of MTB ICL and to screen against Malaysia Nature Product database (NADI) for MTB ICL potential inhibitors. The potential inhibitors from the screening was then is to test with *in vitro* experiment to evaluate their inhibitory potential by *in vitro* experiment.

1.3 Tuberculosis

Tuberculosis (TB) is a lethal infectious disease caused by *Mycobacterium* spp., specifically *Mycobacterium tuberculosis* (MTB), first discovered in 1882 by Robert Koch (Youmans, 1979). MTB spread through air when an infected individual coughs, sneezes and talks. A sneeze with 3,000 nasal droplets would release 10,000 active MTB to the air. (Rinaggio, 2003). These MTB can float in the air by attaching to the dust and remain active in the air for several hours (Russell *et al.*, 2010). Upon infection, these strict aerobic and acid-fast MTB can form tubercles at infected area and cause cellular necrosis, hence tuberculosis (Youmans, 1979).

According to World Health Organization (WHO) Tuberculosis Facts (latest updated in year 2014), one-third of the world population has been infected with TB. A total of 95% TB mortality cases occurred in the developing countries. In Malaysia, Malaysian Health Fact from Ministry of Health Malaysia reported that TB has the highest mortality rate among the infectious diseases. Despite the availability of drugs, TB therapy has been challenged by the long treatment regime which is last from 6 to 24 months, multidrug resistant strains, HIV/AIDS and poverty. Under the premise of no new drug available in the past 40 years, this situation has spurred the urgent search for novel TB drug and its target.

MTB survives in two phases, the replication phase (active TB) and the dormant phase (inactive TB). In these two different phases, MTB utilizes different metabolism pathway for different energy source. MTB consumes the carbohydrate and lipid as sole carbon source in replication and dormant phase, respectively. As these two phases undergo different metabolism pathways, possibility to share common enzyme is rather low. Under this circumstances, to select a common enzyme as the drug target which is

simultaneously important for both survival phase of MTB could be a pipe dream. Current available drugs are targeting at the enzyme involved in replication phase of MTB only, including one of the latest potential drug – TMC207. TMC207 which is currently in phase 2 efficacy study surprisingly showed bactericidal property against dormant MTB (Koul *et al.*, 2008). However, no drug was available for those in dormant phase at the moment.

1.3.1 Tuberculosis infection

MTB can trigger primary infection (acute infection; MTB in replication phase) and also latent infection (persistent infection; MTB in dormant phase). Primary infection can be handled by cell-mediated immune response when MTB starts to replicate (Rinaggio, 2003). Although MTB are slow growing, they are still able to replicate before eliminated by slower cell-mediated immune response. When a patient is infected by MTB, MTB will usually attacks lung cavity to develop pulmonary TB as MTB will be phagocyted by alveolar macrophage when they enter via airways (Mohan, 2004; Russell *et al.*, 2010). As shown in Figure 1.1, when MTB-phagocyted macrophage forms granuloma, the granuloma will undergo differentiation to become a more vascularised structure to mineralize and sterilize the infection (Russell *et al.*, 2010). Otherwise, the granuloma will undergo necrosis under certain circumstances such as HIV-infected or malnutrition, to release the infectious mycobacteria back to the airway (Russell *et al.*, 2009).

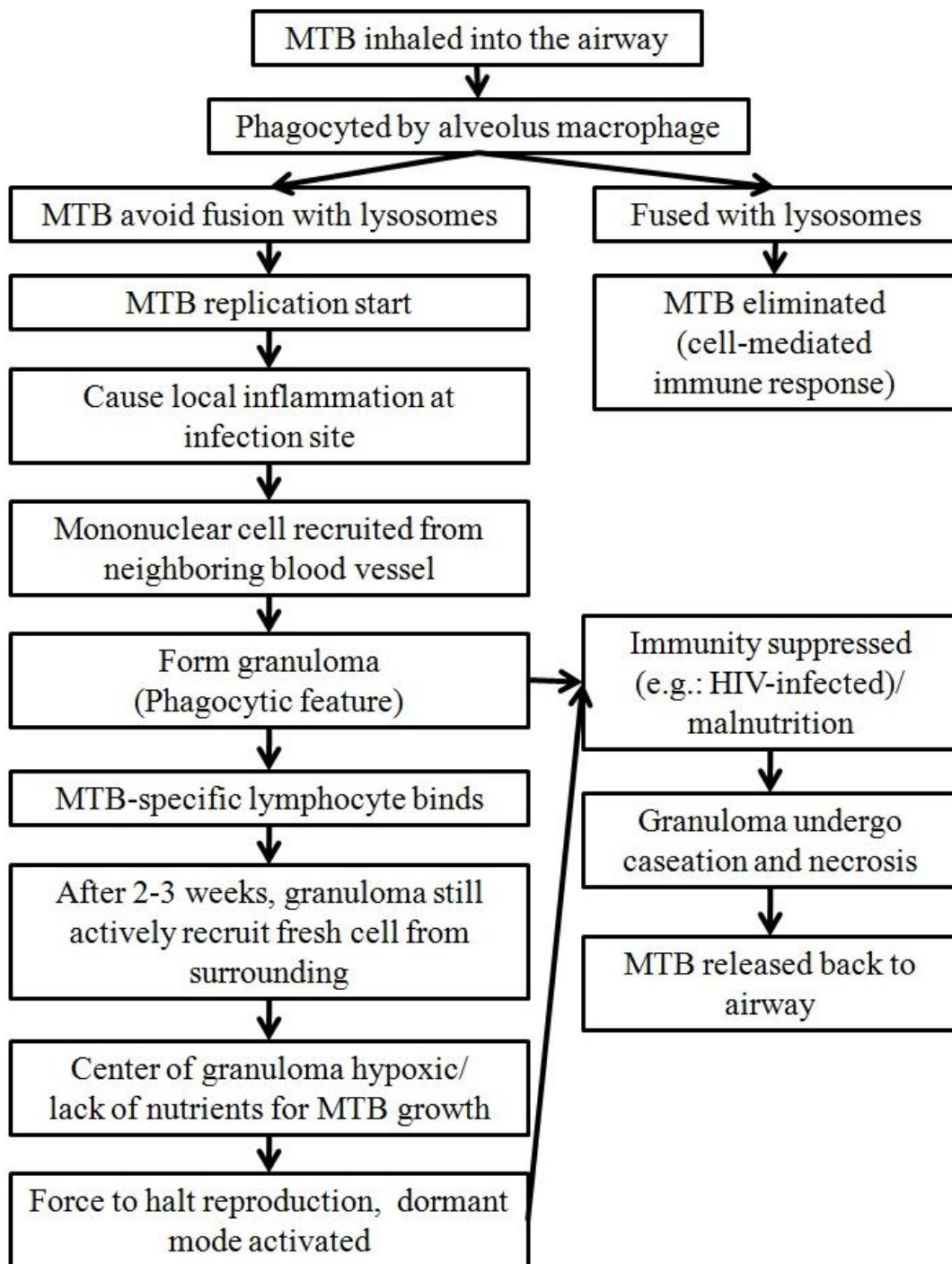


Figure 1.1: Summary of *Mycobacterium tuberculosis* life cycle in human host.

Other than pulmonary TB, extra-pulmonary TB might also occur such as the central nervous system, the lymphatic system, the circulatory system, the genitourinary system, the gastrointestinal system, bones, joints, and even the skin (Mohan, 2004). Other species of *Mycobacterium* such as *Mycobacterium bovis*, *Mycobacterium africanum*, *Mycobacterium canetti*, and *Mycobacterium microti* can also cause TB but they are less common in human (Niobe-Eyangoh *et al.*, 2003). TB patients usually get fatigue easily, losing weight, having fever and night sweat. In more serious cases, symptoms such as coughing, chest pain, coughing out blood-containing sputum, and difficulty in breathing will be observed (Arora, 2009). Further diagnose with chest x-rays, analysis of sputum, and skin tests can be performed to confirm the disease. TB vaccine, Bacillus Calmette-Guérin (BCG) is available and there are also therapeutic TB drugs. To date, tuberculosis had killed more than 1.6 million mankind annually and persisted as latent infection in one-third of the world population (Ranjeet and Vinod, 2008; W.H.O, 2016). As MTB are able to cause persistent infection in immunosuppressed patients, HIV/AIDS population is one of the high risk populations.

1.3.2 Drug resistance of *Mycobacterium tuberculosis*

The therapeutic drugs are divided into first-line drugs and second-line drugs. The first-line drugs are isoniazid, rifampin, ethambutol and pyrazinamide whereas the second-line drugs include streptomycin, kanamycin, ethionamide, para-aminosalicylic acid, ofloxacin, capreomycin, amikacin and cycloserine (Zumla *et al.*, 2013). However, the thick and waxy cell wall of MTB that is rich in novel lipids and polysaccharides formed a challenging barrier for the drugs to reach the respective target. Therefore, the treatment process is no doubt to be lengthy (Baker, 2007). During first six-months treatment using the combination of first-line drugs, MTB will

have sufficient time to establish drug resistance, even though they are extremely slow growing bacteria with doubling time of about 24 hours (Baker, 2007). If the patient could not be cured within the first 6 months, prolonged treatment up to two years with the second-line drug is needed to combat the drug resistant strain (Zumla *et al.*, 2013).

MTB mostly establishes drug resistance through chromosomal mutation (Johnson *et al.*, 2006). When the attack of drugs cause the drug target's gene mutation, the mutated strain (drug resistant strain) will keep replicating with the chromosome. Fortunately, the chromosomal locus that used to resist each drug is different (Johnson *et al.*, 2006). Theoretically, the possibility for wild type MTB to obtain mutation more than two chromosomal loci simultaneously (multidrug resistant strain, MDR) is rather low. Yet, due to the low awareness, the MDR strains manage to be spread. The MDR MTB strain is define as MTB which is resistant to at least both first line drug of isoniazid and rifampin (Johnson *et al.*, 2006). Nowadays, not only MDR strain is getting more prevalence, extensively drug-resistant (XDR) strain that required third line drug (Zumla *et al.*, 2013) and totally drug-resistant (TDR) strain that resist to all first and second line drug is emerging fast (Velayati *et al.*, 2009; Rowland, 2012; Udwardia *et al.*, 2012).

The current available drugs has low efficacy towards MTB in dormancy phase because they target only the drug targets involve replication phase (Getahun *et al.*, 2015). If there is any drug available for dormant MTB in the future, another challenge that can be foreseen is the drug delivery to dormant MTB-containing macrophage which is difficult to identify. As the drug during the dormant phase is still unavailable, the problem of drug resistance during the dormant phase is still unknown.

1.3.3 *Mycobacterium tuberculosis* in dormancy

Replicating MTB located at the macrophage-rich centre of granuloma. When MTB is replicating, granuloma will actively recruits cell. Meanwhile, it is being surrounded by MTB-specific lymphocytes and enclosed by fibrous cuff. When granuloma increases in size, oxygen and nutrients could be hard to transport into the macrophage-rich centre (Russell *et al.*, 2010). It is believed that when the macrophage-rich centre of granuloma become hypoxic or nutrient deprivation, MTB will enter the dormant phase (Gengenbacher *et al.*, 2010). However, it is not an easy task to study the *in vivo* macrophage environment. No work has successfully obtained an *in vivo* model of dormant MTB, only relied on several *in vitro* models. There are two well known *in vitro* models which study dormant MTB with different environment: the Wayne's model (Wayne and Hayes, 1996) and Loebel's model (Betts *et al.*, 2002). Wayne's model studied the dormant MTB behaviour in hypoxic yet nutrient rich medium but Loebel's model used nutrient deprivation yet oxygen rich medium. Although both models have verified the viability of dormant MTB in respective survival environment, no data could actually confirm on which model can represent the real macrophage environment (Gengenbacher *et al.*, 2010).

Dormant phase MTB will be in non-replicating mode. In order to survive within the unfavourable environment in macrophage, MTB shifts its metabolism pathway. One of the obvious change is the carbon source during nutrients deprivation (Betts *et al.*, 2002). Dormant MTB utilizes fatty acid or lipid as their sole carbon source instead of carbohydrate. The energy of MTB is produced via glyoxylate bypass instead of oxygen- dependent tricarboxylic acid cycle (TCA cycle; also known as Krebs cycle) (Singh and Ghosh, 2006). This interesting finding has lead the dormant MTB research to another milestone which is related to glyoxylate bypass.

1.3.4 Isocitrate lyase as drug target

Krebs cycle is a common energy generating pathway if carbohydrate is the main carbon source. However, under nutrient depleted condition, global gene expression of MTB would shut down, including the gene expression for Krebs cycle (Betts *et al.*, 2002). However, gene expression for glyoxylate pathway would not be affected (Gengenbacher *et al.*, 2010). Glyoxylate pathway is a bypass of Krebs cycle or sometimes called the modified Krebs cycle (Dunn *et al.*, 2009). Without ordinary substrate of carbohydrate, nutrient-starved dormant MTB utilizes lipid as the sole carbon source to generate energy.

Figure 1.2 shows the comparison of Krebs cycle and glyoxylate bypass. The early phase of glyoxylate pathway is similar to Krebs cycle. Acetyl-CoA is the only substrate for both glyoxylate and Krebs cycle but the source of acetyl-CoA is different. Carbohydrate has to undergo glycolysis to generate acetyl-CoA for Krebs cycle. Meanwhile, lipid has to undergo beta-oxidation to obtain acetyl-CoA for glyoxylate cycle. The point of divert for these two pathways begin when acetyl-CoA converts into isocitrate. For the glyoxylate pathway, two important enzymes are needed namely isocitrate lyase (ICL) and malate synthase (MS). Isocitrate lyase is responsible to cleave the isocitrate into glyoxylate and succinate whereas malate synthase converts glyoxylate into malate by adding an acetyl group.

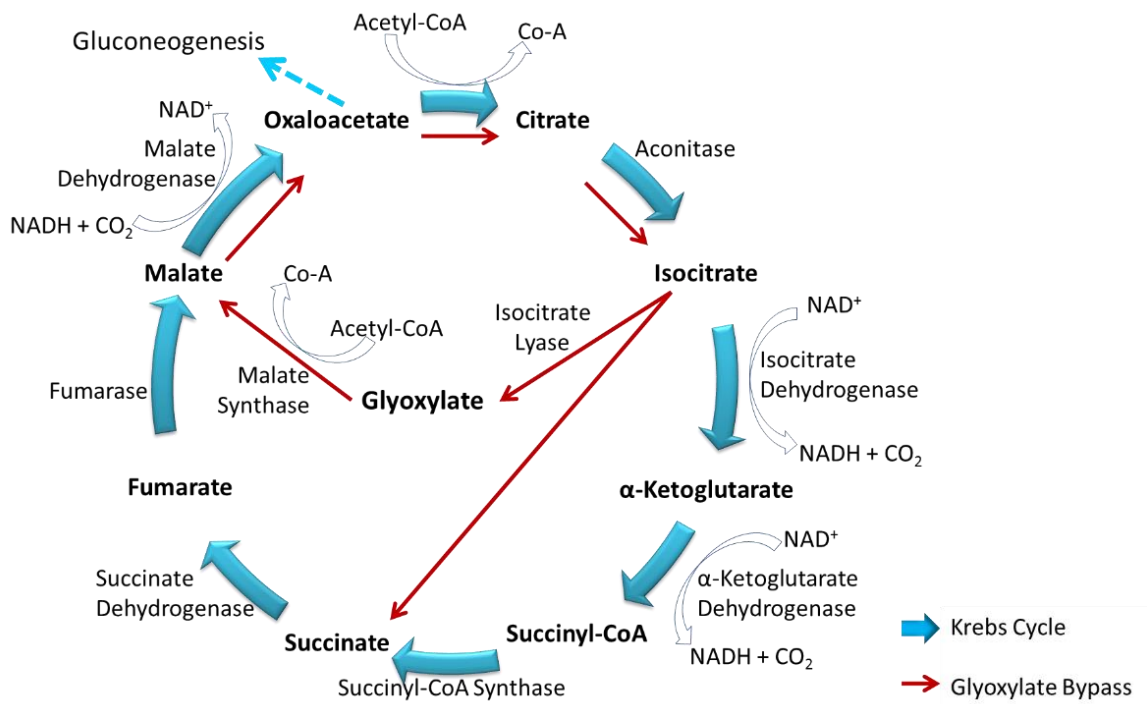


Figure 1.2: The Krebs cycle and the glyoxylate pathway for energy generation. The blue bold arrow indicates the Krebs cycle and the red arrow shows the glyoxylate bypass.

Both ICL and MS were potential drug targets. The drug ability of MS has been proved and various studies have been carried out to optimize its usage (Smith *et al.*, 2003; Kinhikar *et al.*, 2006; Arora, 2009; Krieger *et al.*, 2012). On the other hand, several high throughput screening has been carried out to search for ICL inhibitor at the same time. It was found that its drug availability is not as good as MS. One explanation found regarding the cavity size of the active site. ICL active site is relatively small in capacity compared with that of MS (Krieger *et al.*, 2012; Sharma *et al.*, 2000). Other than this, not much research has been published to further explain about the low drug availability of ICL. This has incited the interest in this study to understand ICL.

1.3.5 Isocitrate lyase related studies

The structure of MTB ICL in Figure 1.3 was solved in year 2000 by Sharma *et al.* They reported that ICL is stable as dimers but functional in tetramer. Each of the subunits has an unusual α/β barrel as the largest core domain which is formed by of eight α -helix and β -strand respectively. Each subunit has an extra helix that projected out from the barrel and another two ensuing helix involved in the interaction among the subunits. On top of the barrel, there is an important small β -domain which has several active side residues.

There are a total of three ICL structures solved by Sharma *et al.*(2000). The first structure is a ligand-free ICL which is in “open conformation” (PDB id: 1F61). When ligand glyoxylate and succinate (PDB id: 1F8I); or pyruvate (PDB id: 1F8M) binds, they trigger a conformational change to make the ICL shift into a “close conformation”. ICL is an enzyme that is able to perform reversible catalysis of

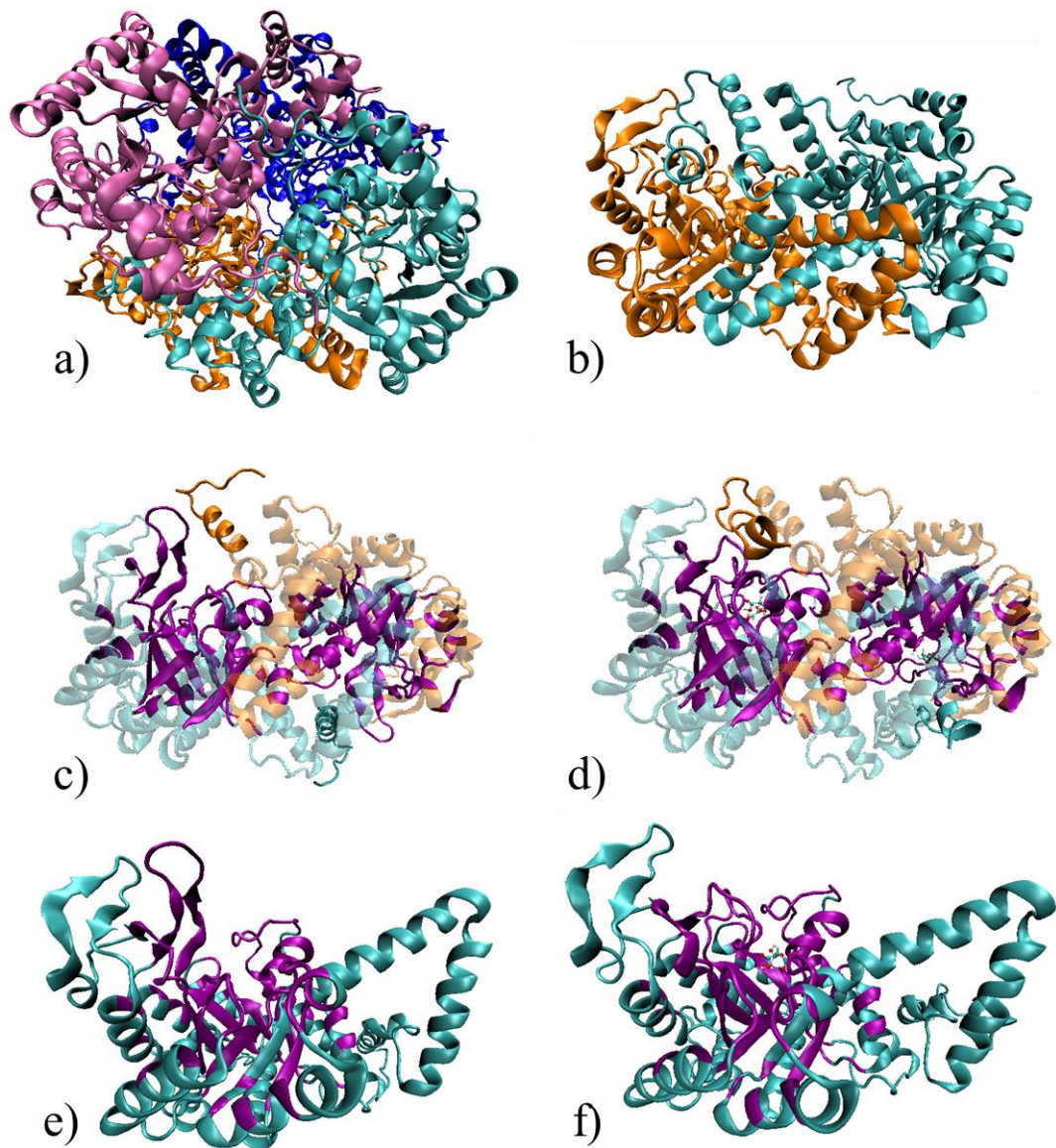


Figure 1.3: The structure of ICL from MTB. a) Tetramer, each colour represents a subunit of ICL; b) dimer, cyan and orange represents monomer 1 and monomer 2; c) dimer in open conformation; d) ICL dimer in close conformation; e) monomer 1 in open conformation without ligand; and e) monomer 1 in close conformation with ligand. Purple represents the active site (Sharma *et al.*, 2000; Lee *et al.*, 2015).

isocitrate, meaning that it is able to cleave as well as form isocitrate. However, no study has been published on the interaction between the ICL and isocitrate. The catalytic mechanism of forming isocitrate from glyoxylate and succinate was only partly described (Sharma *et al.*, 2000). The cleavage mechanism of isocitrate to produce glyoxylate and succinate is remain unknown.

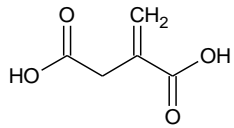
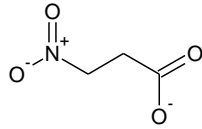
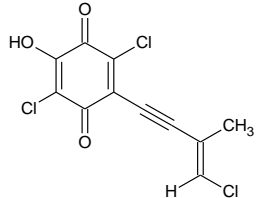
According to Dunn *et al.* (2009), ICL gene is not found in any placental mammals. Muñoz-Elías and McKinney (2005), showed that there are 2 types of ICL exist in MTB: the ICL 1 (prokaryotic-like isoform) and ICL 2 (eukaryotic-like isoform). ICL1 and ICL2 are jointly required for MTB. Absence of either one of them causes little effect for MTB but absence of both will cause MTB being eliminated from the lungs. Gould *et al.*(2006) reported that ICL 1 has dual roles. ICL 1 is needed in both glyoxylate cycle and methylcitrate cycle in MTB. Methylcitrate cycle is a cycle that removes the by-product of lipid beta-oxidation, the propionyl-CoA, which is toxic to MTB. In this cycle, 3 enzymes needed are methylcitrate synthase, methylcitrate dehydrogenase and 2-methylisocitrate lyase (MCL). It was found that MTB only produces methylcitrate synthase and methylcitrate dehydrogenase but not MCL. The function of MCL was carried out by ICL 1. This study has thus shown that ICL is more important than expected (Gould *et al.*, 2006).

Another research topic highlighted is the screening of inhibitor of ICL. According to the review by Dunn *et al.*(2009), the well-known ICL inhibitors include itaconate, 3-nitropropionate, 3-bromopyruvate, malate and oxalate (Bentrup *et al.*, 1999; McFadden and Purohit, 1977). Most of the inhibitors were analog of the natural substrate. However, they were later proven toxic and non-specific to develop into drug as they will inhibit some of the important metabolism enzymes which are simultaneously exist in both human and MTB. For instance, one of the succinate

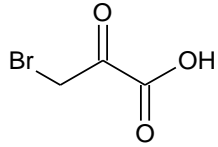
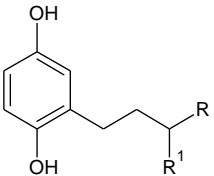
analogs, 3-nitropropionate cause neurotoxicity (Greene *et al.*, 1998). Another succinate analog, itaconate affect the growth of rat (Booth *et al.*, 1952) and also cause hypertonicity for cat's blood pressure (Finkelstein *et al.*, 1947). Whereas, the analog of glyoxylate, 3-bromopyruvate is an energy blocker (Ko *et al.*, 2004; Shoshan, 2012).

There are a few high throughput screening of ICL were reported. Two groups have reported their works in year 2006. First project is carried out by Global Alliance for TB Drug Development and GlaxoSmithKline, extensively screen for ICL inhibitor via high throughput screening. However, the project was terminated as the outcome was modestly successful (Global Alliance For TB Drug Development, 2010) In the same year, a Chinese group searched for potential ICL inhibitors from traditional Chinese medicine. They concluded that extracts form *Illicium verum* and *Zingiber officinale* were able to inhibit ICL (Bai *et al.*, 2006). Unfortunately, the lead compound for ICL inhibition is remains unknown. In later years, the searching efforts continued by some groups with their respective in house chemical compound library. Their HTS managed to identify lead compound I2906 (Lu *et al.*, 2010), Ydcm67 (Ji *et al.*, 2011) and IMBI-3 (Liu *et al.*, 2016) as the potential inhibitor for ICL. More ICL potential inhibitors that was screened with various strategies such as using MTB ICL and non-MTB ICL as well as screening from natural compound or synthetic compound were summarized in a Table 1.1 (Lee *et al.*, 2015).

Table 1.1: Summary of synthetic and natural potential inhibitor for MTB ICL and non-MTB ICL.

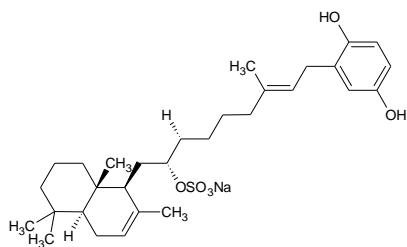
No.	Published Year	Inhibitor	Source	Description	Target ICL	Inhibition* (IC ₅₀)	Remarks
1	1977	<p>Itaconate (McFadden and Purohit, 1977; Bentrup <i>et al.</i>, 1999)</p> 	Synthetic	Succinate analog	<i>Pseudomonas indigofera</i>	K _i = 120	Established inhibitor
2	1982	<p>3-nitropropionate (Schloss and Cleland, 1982; Bentrup <i>et al.</i>, 1999)</p> 	Synthetic	Succinate analog	<i>Pseudomonas indigofera</i>	K _i = 120	Established inhibitor
3	1990	<p>Mycenon (Hautzel <i>et al.</i>)</p> 	<i>Mycena</i> sp.	Fungi	<p><i>Acinetobacter calcoaceticus</i></p> <p><i>Neurospora crassa</i></p> <p><i>Ricinus communis</i></p>	<p>5.2 μM</p> <p>7.4 μM</p>	No information on positive control

3-bromopyruvate (Ko and McFadden, 1990; Bentrup *et al.*, 1999)

4	1990		Synthetic	Glyoxylate analog	<i>Escherichia coli</i>	3 μ M	Established inhibitor
5	2005	DNAzyme (Li <i>et al.</i> , 2005)	Synthetic	-	<i>Mycobacterium tuberculosis</i>	-	
6	2006	Extract of Traditional Chinese Medicine (Bai <i>et al.</i>)	<i>Zingiber officinale</i> , <i>Illicium verum</i>	Plant	<i>Mycobacterium tuberculosis</i>	47.7 μ g/ml 18.2 μ g/ml	Positive control IC ₅₀ of itaconate = 90 μ g/ml (Good inhibitory)
Hydroquinone derivatives (Yang <i>et al.</i>)							
7	2007		Synthetic	-	<i>Candida albicans</i>	0.28-1.02 mM	Positive control IC ₅₀ of itaconate = 0.06 mM (Weak inhibitory)

Halisulfate 1 (Shin *et al.*, 2007; Lee *et al.*, 2007b)

8 2007



Hippospongia sp.

Marine sponge

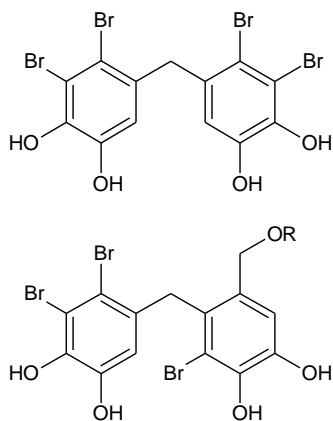
Magnaporthe grisea

12.6 μM

No information on positive control
(High inhibitory)

Bromophenols (Lee *et al.*)

9 2007



Odonthalia corymbifera

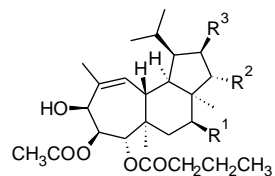
Red algae

Magnaporthe grisea

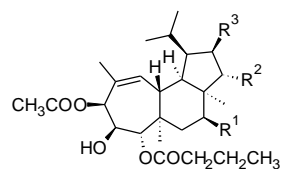
2.0 – 2.8 μM

Positive control
IC₅₀ of
3-nitropropionate
= 94.2 μM
(High inhibitory)

Polyoxygenated diterpenes (Jang *et al.*)



10 2008



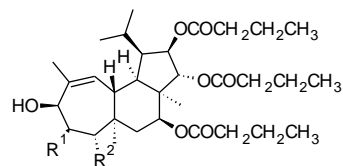
Phorbas sp.

Marine sponge

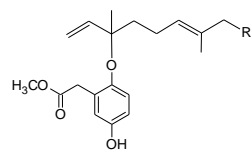
-

LC₅₀ of
55 - 140 µg/ml

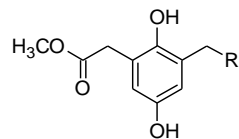
No information on
positive control
(Weak inhibitory)



Meroditerpenoids (Jung *et al.*)



11 2008



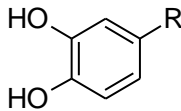
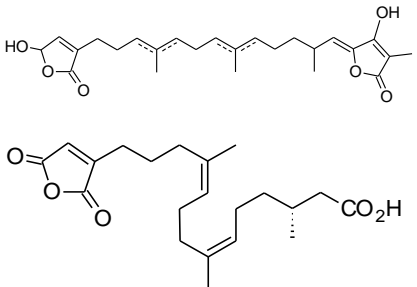
Sargassum
siliquastrum

Brown algae

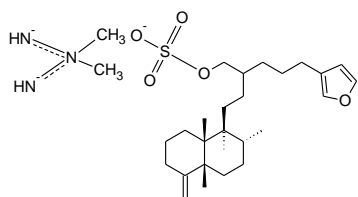
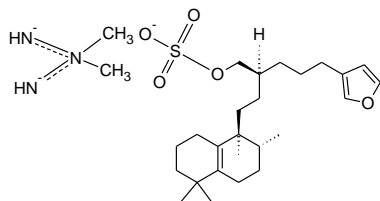
Candida albicans

50 – 95 µg/ml

No information on
positive control
(Weak inhibitory)

12	2008	<p>Dihydroxystyrene metabolites (Chang <i>et al.</i>)</p> 	Association of <i>Poecillastra wondoensis</i> and <i>Jaspis</i> sp.	Marine sponge	<i>Candida albicans</i>	28.7 to >200 $\mu\text{g/ml}$	<p>Positive control IC_{50} of itaconate = 5.8 $\mu\text{g/ml}$ (Weak to moderate inhibitory)</p>
13	2008	<p>Sesterterpenoids (Wang <i>et al.</i>)</p> 	<i>Sarcotragus</i> sp.	Marine sponge	<i>Candida albicans</i>	12.5 – 19.9 $\mu\text{g/ml}$	<p>Positive control IC_{50} of Itaconate = 4.9 $\mu\text{g/ml}$ (Moderate to high inhibitory)</p>

Sesterterpene sulphates (Lee *et al.*)



14 2008

Dysidea sp

Marine sponge

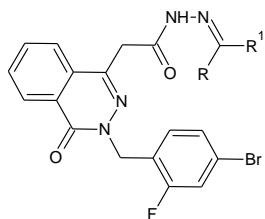
Candida albicans

31.3 – 33.8 μ M

Positive control IC_{50}
of 3-nitropropionate
= 50.7 μ M

(High inhibitory)

Phthalazinyl derivatives (Sriram *et al.*, 2009)



15 2009

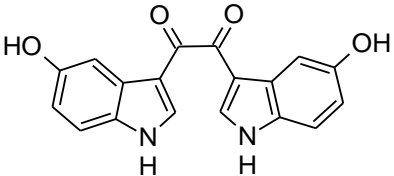
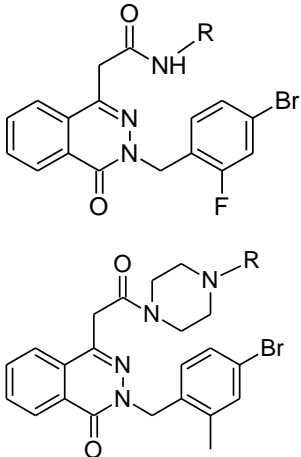
Synthetic

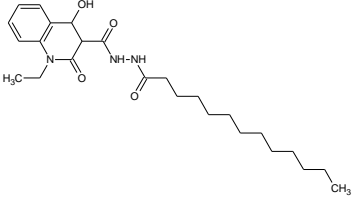
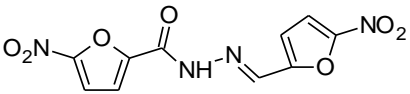
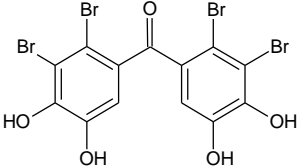
-

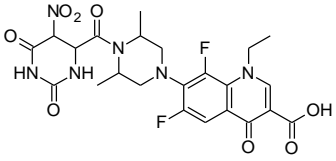
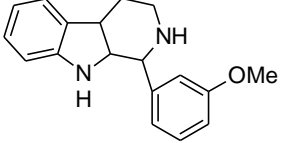
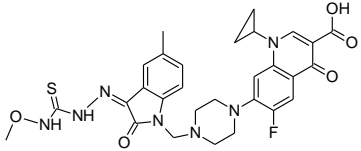
Mycobacterium tuberculosis

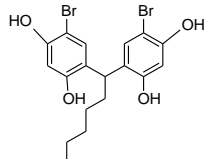
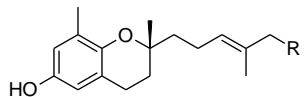
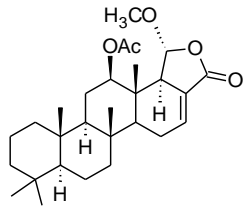
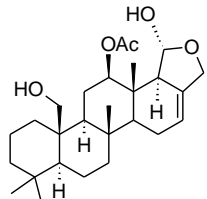
45 – 61%
inhibition at 10
 μ M

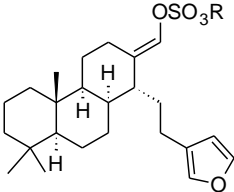
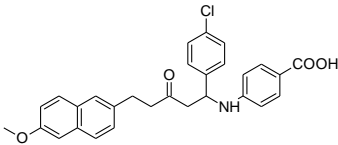
Positive control
3-nitropropionate has
63.2% inhibition at
100 μ M

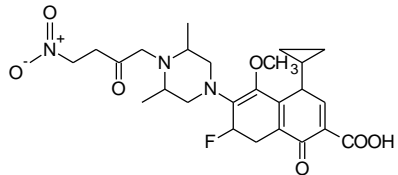
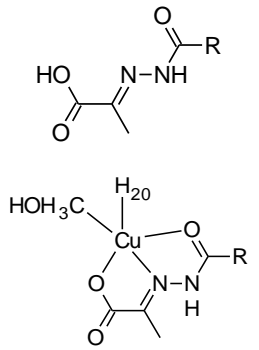
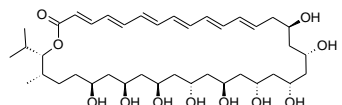
16	2009	<p>Hyrminos B (Lee <i>et al.</i>)</p> 	<i>Hyrminos</i> sp.	Marine sponge	<i>Candida albicans</i>	89 μ M	<p>Positive control IC_{50} of 3-nitropropionate = 50.7 μM (High inhibitory)</p>
17	2010	<p>Phthalazin-4-ylacetamide (Sriram <i>et al.</i>, 2010b)</p> 	Synthetic	-	<i>Mycobacterium tuberculosis</i>	40.62 – 66% inhibition at 10 μ M	<p>Positive control 3-nitropropionate has 68.2% inhibition at 100 μM</p>

18	2010	<p>Extract of Traditional Chinese Medicine (I2906) (Lu <i>et al.</i>, 2010)</p> 	-	Plant	<i>Mycobacterium tuberculosis</i>	134 µg/ml	Control samples were untreated samples
19	2010	<p>5-Nitro-2-furoic acid hydrazones with furan-2-carbaldehyde (Sriram <i>et al.</i>, 2010c)</p> 	Synthetic	-	<i>Mycobacterium tuberculosis</i>	86.8% inhibition at 10 mM	<p>Positive control 3-nitropropionate has 63.2% inhibition at 100 µM</p> <p>(Good inhibitory)</p>
20	2010	<p>Bromophenols (Oh <i>et al.</i>)</p> 	Synthetic	-	<i>Candida albicans</i>	2.65 µM	<p>Positive control IC₅₀ of 3-nitropropionate = 50.7 µM</p> <p>(High inhibitory)</p>

21	2010	<p>5-Nitro-2,6-dioxohexahydro-4-pyrimidinecarboxamides (Sriram <i>et al.</i>, 2010a)</p> 	Synthetic	-	<i>Mycobacterium tuberculosis</i>	45.7% inhibition at 10 mM	<p>Positive control 3-nitropropionate has 68.2% inhibition at 100 μM</p> <p>(Good inhibitory)</p>
22	2010	<p>Indole-containing natural compound (analog) (Lee <i>et al.</i>)</p> 	Synthetic	-	<i>Candida albicans</i>	75 μM	<p>Positive control IC₅₀ of 3-nitropropionate = 50 μM</p> <p>(High inhibitory)</p>
23	2010	<p>Isatinyl thiosemicarbazones derivatives (Banerjee <i>et al.</i>, 2011)</p> 	Synthetic	-	<i>Mycobacterium tuberculosis</i>	63.44% inhibition at 10 mM	<p>Positive control 3-nitropropionate has 65.9% inhibition at 100 mM</p> <p>(Good inhibitory)</p>

24	2011	<p>Brominated resorcinol dimer (Bouthenet <i>et al.</i>)</p> 	Synthetic	-	<i>Candida albicans</i>	28 μ M	<p>Positive control IC₅₀ of 3-nitropropionate = 6.0 μM (Good inhibitory)</p>
25	2011	<p>Sargachromanols (Chung <i>et al.</i>)</p> 	<i>Sargassum siliquastrum</i>	Brown algae	<i>Candida albicans</i>	118.4 – 172.9 μ M	<p>Positive control IC₅₀ of 3-nitropropionate = 34.8 μM (Moderate inhibitory)</p>
26	2011	<p>Scalarane Sesterterpenes (Jeon <i>et al.</i>)</p>  	<i>Hyatella</i> sp.	Marine sponge	<i>Candida albicans</i>	40.8 – 55.3 μ M	<p>Positive control IC₅₀ of 3-nitropropionate = 27.9 μM (Weak inhibitory)</p>

27	2011	Suvanine salt (Bae <i>et al.</i>) 	<i>Coscinoderma</i> sp.	Marine sponge	<i>Candida albicans</i>	5 – 17 μ M	Positive control IC ₅₀ of 3-nitropropionate = 27.9 μ M (Moderate inhibitory)
28	2011	Chelerythrine extract (Liang <i>et al.</i>)	<i>Chelidonium majus</i>	Plant	<i>Mycobacterium tuberculosis</i>	Expression level decreased 5 fold	-
29	2011	Mannich base, Ydcm67 (Ji <i>et al.</i>) 	Synthetic	-	<i>Mycobacterium tuberculosis</i>	57.4% inhibition at 0.05mg/ml	Positive control oxalic acid has 95.55% inhibition at 0.05M
30	2011	Peptide inhibitor (Yin <i>et al.</i>)	Synthetic	-	<i>Mycobacterium tuberculosis</i>	Inhibition rate 38.2 – 47.92%	Samples contain no peptide inhibitor or ICL in reaction system as controls

31	2011	<p>3-nitropropionamides derivatives (Sriram <i>et al.</i>)</p> 	Synthetic	-	<i>Mycobacterium tuberculosis</i>	0.1 μ M	<p>Positive control IC₅₀ of 3-nitropropionate = 116.0 μM (Good inhibitory)</p>
32	2012	<p>Pyruvate-isoniazid analog with their copper complex (Shingnapurkar <i>et al.</i>)</p> 	Synthetic	-	<i>Mycobacterium tuberculosis</i>	Inhibition rate 6 – 92 %	Control docking using pyruvic acid
33	2012	<p>Bahamaolides A (Macrolide) (Kim <i>et al.</i>)</p> 	<i>Streptomyces</i> sp.	Actinomycete (Actinobacteria)	<i>Candida albicans</i>	10.8 μ M	<p>Positive control IC₅₀ of 3-nitropropionate = 20.1 μM (High inhibitory)</p>